(U) Miniaturized Nanocomposite Piezoelectric Microphones for UAS Applications

October 22, 2012

Stephen Horowitz, Jon Fox, Dustin Mathias, Jean Cortes, Michael Allen, Laura Barkett
Ducommun Miltec, Emerging Technologies Group, Huntsville AL 35773

and

Mohan Sanghadasa
US Army – AMRDEC, Redstone Arsenal, AL 35898

ABSTRACT

Recent advances in microfabrication and nanoscale material synthesis have enabled a new generation of sub-mm piezoelectric microphones with the sensitivity of larger acoustic sensors. The piezoelectric approach enables new applications and platforms such as collision avoidance on UAS due to environmental damage resistance, small size, ability to flush mount and zero power supply requirements. In this paper we will present our latest development efforts to incorporate nanostructured piezoelectric material into a working microfabricated microphone. Further, we will discuss the unique challenges that must be overcome to package these sensors in arrays for a UAS platform.

This paper presents the latest results from our development efforts. Utilizing lumped element and finite element modeling and composite material analysis, we designed a series of microphones with diameters ranging from 100 um to 800 um. A microfabrication process flow that incorporates a technique for integrating ZnO nanorods into a polymer diaphragm was then developed. Sensors were fabricated, released, and packaged on printed circuit boards in preparation for acoustic and electrical testing. Preliminary tests indicate successful fabrication with a flexible diaphragm, consistent electrical properties (dielectric constant and loss tangent) and measureable piezoelectric activity. Sensor characterization results show performance in line with theoretical predictions. Additional tests are currently underway using specially designed test structures to quantify material parameters such as Young's modulus, density and residual stress.

Keywords: Piezoelectricity, microphones, acoustic sensors, nanostructures, MEMS, composite materials, microfabrication, nanorods

Report Documentation Page

Form Approved
OMB No. 0704-0188

1. REPORT DATE	2. REPORT TYPE	3. DATES COVERED
OCT 2012	**N/A**	**-**

4. TITLE AND SUBTITLE
Miniaturized Nanocomposite Piezoelectric Microphones for UAS Applications

5a. CONTRACT NUMBER
5b. GRANT NUMBER
5c. PROGRAM ELEMENT NUMBER

6. AUTHOR(S)

5d. PROJECT NUMBER
5e. TASK NUMBER
5f. WORK UNIT NUMBER

7. PERFORMING ORGANIZATION NAME(S) AND ADDRESS(ES)
Ducommun Miltec, Emerging Technologies Group, Huntsville AL 35773

8. PERFORMING ORGANIZATION REPORT NUMBER

9. SPONSORING/MONITORING AGENCY NAME(S) AND ADDRESS(ES)

10. SPONSOR/MONITOR'S ACRONYM(S)
11. SPONSOR/MONITOR'S REPORT NUMBER(S)

12. DISTRIBUTION/AVAILABILITY STATEMENT
Approved for public release, distribution unlimited

13. SUPPLEMENTARY NOTES
See also ADM202976. 2012 Joint Meeting of the Military Sensing Symposia (MSS) held in Washington, DC on October 22-25, 2012.

14. ABSTRACT

Recent advances in microfabrication and nanoscale material synthesis have enabled a new generation of sub-mm piezoelectric microphones with the sensitivity of larger acoustic sensors. The piezoelectric approach enables new applications and platforms such as collision avoidance on UAS due to environmental damage resistance, small size, ability to flush mount and zero power supply requirements. In this paper we will present our latest development efforts to incorporate nanostructured piezoelectric material into a working microfabricated microphone. Further, we will discuss the unique challenges that must be overcome to package these sensors in arrays for a UAS platform. This paper presents the latest results from our development efforts. Utilizing lumped element and finite element modeling and composite material analysis, we designed a series of microphones with diameters ranging from 100 um to 800 um. A microfabrication process flow that incorporates a technique for integrating ZnO nanorods into a polymer diaphragm was then developed. Sensors were fabricated, released, and packaged on printed circuit boards in preparation for acoustic and electrical testing. Preliminary tests indicate successful fabrication with a flexible diaphragm, consistent electrical properties (dielectric constant and loss tangent) and measureable piezoelectric activity. Sensor characterization results show performance in line with theoretical predictions. Additional tests are currently underway using specially designed test structures to quantify material parameters such as Youngs modulus, density and residual stress.

15. SUBJECT TERMS

16. SECURITY CLASSIFICATION OF:			17. LIMITATION OF ABSTRACT	18. NUMBER OF PAGES	19a. NAME OF RESPONSIBLE PERSON
a. REPORT	b. ABSTRACT	c. THIS PAGE			
unclassified	**unclassified**	**unclassified**	**SAR**	**14**	

1.0 Introduction

1.1. Motivation

Piezoelectric microphone miniaturization is paving the way towards new applications and platforms, such as UAS collision avoidance. Such systems require compact, flush mounted arrays that can withstand the environment. Achieving high sensitivity and low noise in an acoustic sensor, however, becomes more challenging as the sensor size is reduced.

Historically, miniaturization of piezoelectric microphones has progressed along two fronts: 1) high mechanical sensitivity via thin flexible diaphragms and 2) high mechanical-to-electrical coupling via strongly piezoelectric materials [1–4]. Continued reductions in scale, however, have been hampered by the lack of materials that simultaneously satisfy both criteria [5].

In previous efforts, we explored the fabrication limits of piezoelectric microphone miniaturization using conventional piezoelectric materials [5]. Further reduction in size was found to be hampered by residual stress and high stiffness that limited microphone sensitivity. To overcome these limitations, we began developing a novel composite material that exhibited piezoelectric behavior while maintaining a low stiffness and residual stress and could be fabricated into ultrathin diaphragms.

1.2. Challenges

The UAS platform imposes a set of unique challenges and constraints on microphone development. Acoustic sensing inherently requires contact with the environment. Unfortunately, rain, fog, wind, vibration and temperature extremes may all be present on a UAS exterior. The majority of commercially available miniature microphones employ some form of capacitive transduction: either an electret or condenser type. Capacitive transduction though is sensitive to moisture and vibration because a very small gap must be maintained between the acoustic diaphragm and an electrode backplane for proper signal transduction. Temperature variation also affects sensor performance, due to differences in thermal coefficients of expansion and the resulting induced stresses. Furthermore, flow-induced noise is a concern for any exposed acoustic sensor.

Apart from the environment, the UAS platform imposes additional constraints on power and size. For microphones on aerosurfaces, the sensors need to be flush mounted to avoid generating additional flow-induced noise.

1.3. Paper Overview

This paper continues in Section 2 with an overview of the design concept, followed in Section 3 by theoretical modeling of the sensor. Section 4 then addresses the fabrication of the devices, followed in Section 5 with characterization including details on the measurement setup and results.

2.0 Design

2.1. Concept

As microphone dimensions are reduced, sensitivity tends to decrease due to physical scaling effects, leading to a reduced ability to detect faint signals. Our design compensates for these geometric scaling effects through increased aspect ratio structures and improved material properties. We combine a highly compliant polymer as the structural diaphragm with embedded zinc oxide (ZnO) nanorods for high piezoelectric transduction ability. The combination retains much of the compliance of the polymer while still offering high piezoelectric transduction sensitivity. Furthermore, we are able to tailor the material properties through minor adjustments of the nanorod to polymer concentrations.

Top and side view schematics of the microphone are shown in Figure 1. The sensor consists of a circular, flexible nanocomposite piezoelectric diaphragm with ring-shaped top electrodes. A ring-shaped electrode was used to limit charge capture to the region of highest strain, near the clamped edge. Four different designs were explored, from modeling through fabrication and characterization, ranging in size from a 50 μm radius to a 400 μm radius. All sensors were designed and fabricated with a 1 μm thick composite layer. The geometric specifications for each of the four designs are listed in Table 1.

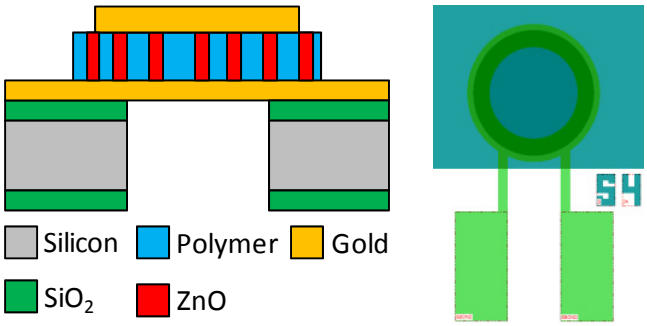

Figure 1: Side and top view schematics of the nanocomposite piezoelectric microphone.

Table 1: Geometric specifications for four microphone designs

Design	Inner Radius	Outer Radius
1	37.5 µm	50 µm
2	75 µm	100 µm
3	150 µm	200 µm
4	300 µm	400 µm

3.0 Theory

In order to accurately predict the performance of the microphones, it is necessary to combine a lumped element sensor model with a composite material model The composite model is first used to determine the relevant material properties of the composite material via analytical modeling. These material properties are then used as parameters to compute lumped element values in an equivalent circuit representation. System dynamics and performance can then be calculated.

3.1. Composite Material Modeling

The composite piezoelectric material used for the diaphragm exhibits properties that depend on the relative concentrations of the two components that comprise the material. It is precisely for this reason that we chose to use such a material for a sensor. By tailoring the relative concentrations, we can achieve a material with a high compliance and decent piezoelectric properties. The material consists of vertically aligned ZnO nanorods in a SU-8 polymer matrix. The intent was to capture the piezoelectric behavior of the ZnO nanorods while leveraging the low elastic modulus of the polymer to maintain a low stiffness.

Combining two materials to form a composite material does not necessarily generate properties that are linearly proportional to their respective concentrations (i.e. the rule of mixtures). In fact, the material properties can have a complex dependence on the inclusion concentration or volume fraction, *Phi* .

Analytical models have been developed and expanded by a number of researchers for spherical piezoelectric properties over a large range of volume fractions [6], [7]. While our inclusions are elongated nanorods, we used the spherical inclusion models as a first-pass approximation to guide our design. For our composite material, consisting of ZnO nanorods in an SU-8 matrix, we computed Young's modulus, relative permittivity and the piezoelectric coefficients, d_{31} and d_{33}. The analytical models employed here are only valid up to a volume fraction of 0.7 [6] and we restricted plotting and analysis of our composite to that range as a result.

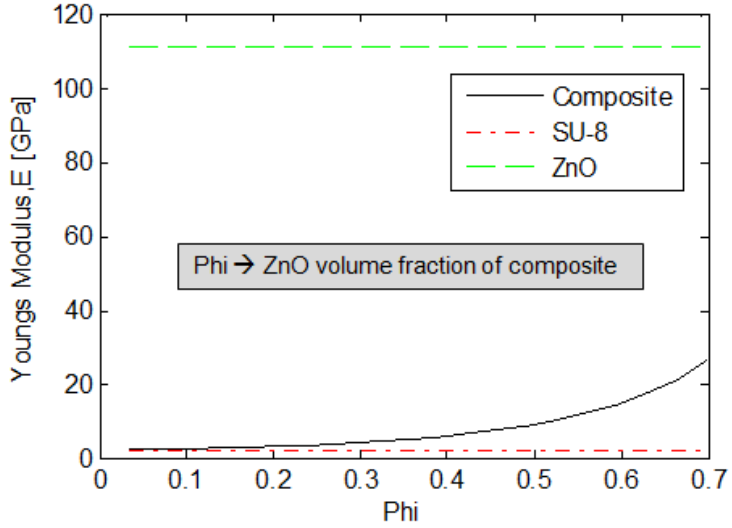

Figure 2: Young's modulus computed as a function of volume fraction, *Phi*, overlaid with the values for the constituent materials.

As can be seen in Figure 1, the Young's modulus of the composite is not linearly dependent on the volume fraction. Instead, it exhibits relatively soft behavior, i.e. low modulus, over much of the computed volume fraction range. The Young's modulus is predicted to exhibit only 9% of the maximum value (the value of the ZnO inclusions) at a volume fraction of 0.5.

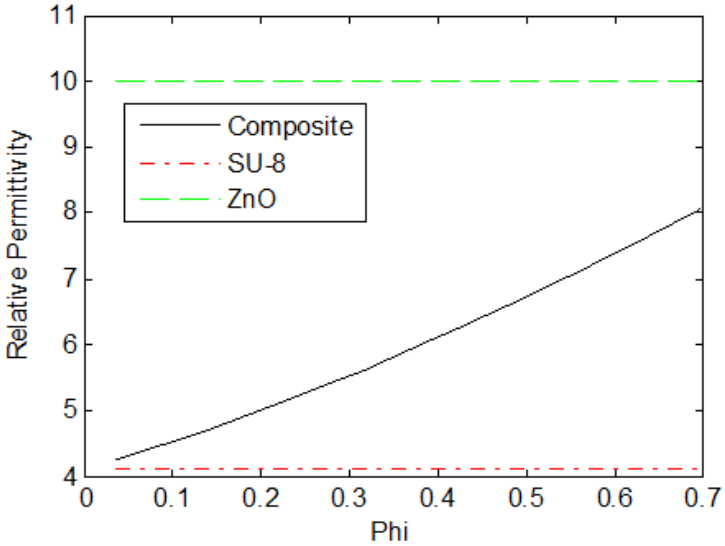

Figure 3: Relative permittivity computed as a function of volume fraction, *Phi*, overlaid with the values for the constituent materials.

Figure 2 shows the relative permittivity, i.e. dielectric constant, over the same range of volume fraction. In contrast to the Young's modulus, the permittivity varies nearly linearly, reaching halfway between the values of the constituent materials at a volume fraction of 0.5.

The transverse and longitudinal piezoelectric coefficients, d_{31} and d_{33}, are plotted in Figure 3 and Figure 4. They both vary somewhat linearly at low volume fractions, but rapidly increase and start to saturate near the coefficient values of the piezoelectric inclusion, achieving 72% of full value at a volume fraction of 0.5. Thus we see that over much of the practicable range of volume fraction, we can expect to achieve a low Young's modulus but still have relatively high piezoelectric coefficients.

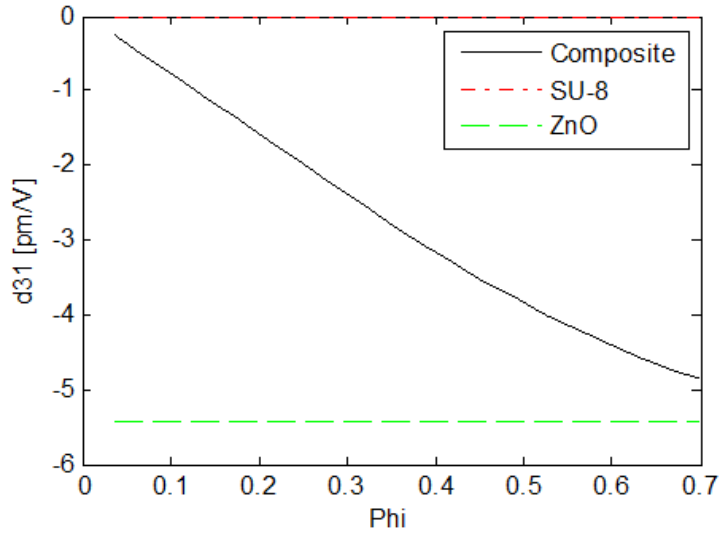

Figure 4: Transverse piezoelectric coefficient, d_{31}, computed as a function of volume fraction, *Phi*, overlaid with the values for the constituent materials.

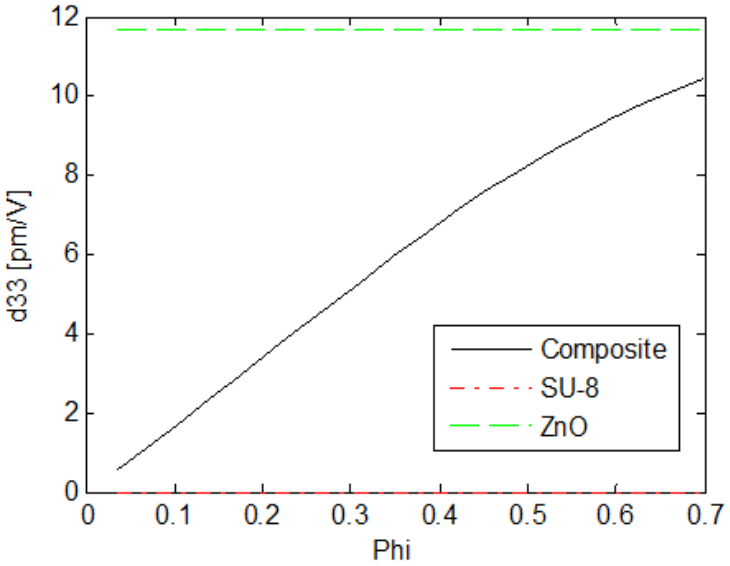

Figure 5: Longitudinal piezoelectric coefficient, d_{33}, computed as a function of volume fraction, *Phi*, overlaid with the values for the constituent materials.

3.2. Lumped Element Modeling (LEM)

Using a lumped element, equivalent circuit model of a piezoelectric microphone, we are able to predict sensor performance specifications, such as sensitivity or minimum detectable signal (MDS). Details of lumped element modeling of a circular piezoelectric microphone are beyond the scope of this paper and are provided elsewhere [8]. Shown in Figure 5 is a plot of the predicted microphone sensitivity as a function of the volume fraction for three different materials: ZnO/SU-8 composite, ZnO thin film, and PZT thin film. This was computed for a microphone of outer radius, $R_2 = 400\mu m$, and a thickness $t = 1\mu m$. Note the significant increase in sensitivity compared to a solid ZnO or PZT film. This arises because, as shown above, the piezoelectric coefficient rises rapidly for even small volume fractions, whereas the Young's modulus remains low over much of the predicted range. An optimal volume fraction of 0.3 yielded a 17-fold increase in sensitivity over ZnO and a 49-fold increase over PZT.

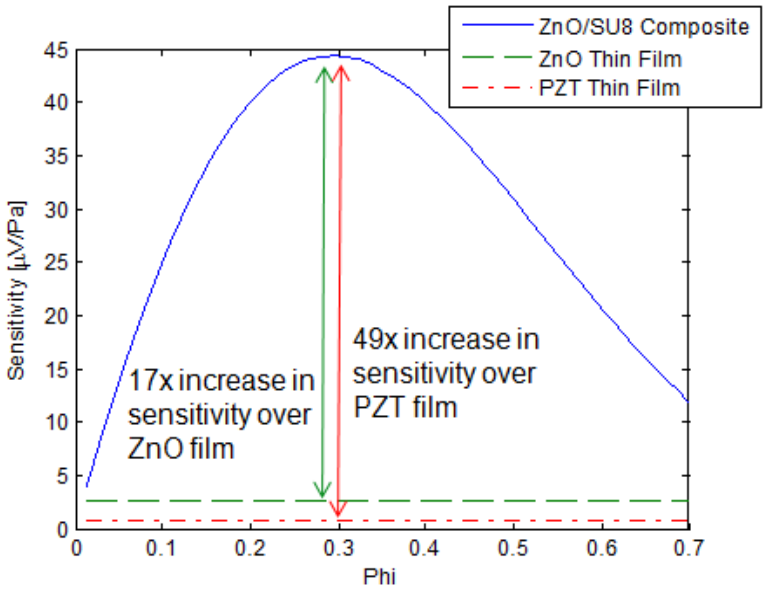

Figure 6: Microphone sensitivity as a function of volume fraction computed for the composite film and compared against thin films of ZnO and PZT.

3.3. Predicted Performance

Using the lumped element and composite material models described previously, we predicted the sensitivity (Figure 7) and minimum detectable signal (MDS) (Figure 8) of four different sensor sizes and two different diaphragm thicknesses. We had originally intended to fabricate devices with a diaphragm thickness of 200 nm; however, during our initial fabrication run, we have been limited to a minimum thickness of 1 μm. Predictions for both are shown here to illustrate what we can currently achieve as well as what we think can achieve with improvements in the fabrication process.

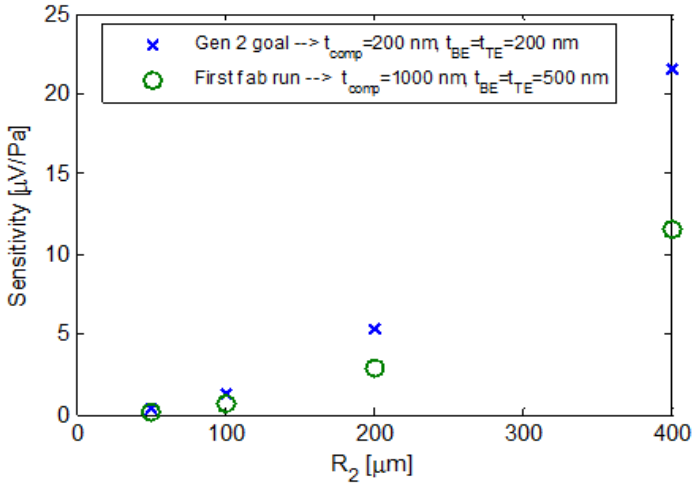

Figure 7: Predicted microphone sensitivity for four different sensor sizes and two different diaphragm thicknesses.

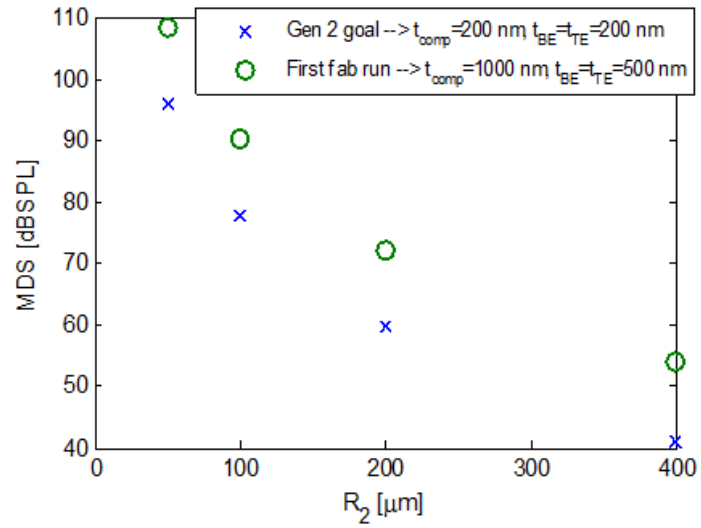

Figure 8: Predicted microphone MDS for four different sensor sizes and two different diaphragm thicknesses.

4.0 Fabrication and packaging

4.1. Process flow

Fabrication of the sensors was performed using a combination of standard thin film, microfabrication processes and an internally developed, low-temperature procedure for integrating vertically aligned ZnO nanorods into a thin polymer film. The result is a relatively simple, high-yield process for generating large quantities of piezoelectric microphones with low-stress composite diaphragms. Figure 7 shows a condensed process flow diagram for creating the microphones.

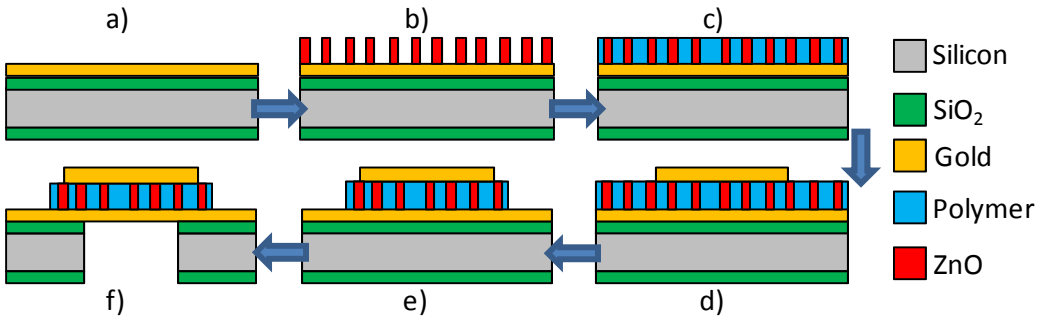

Figure 9: Condensed fabrication process flow- a)Grow thermal oxide and deposit gold for bottom electrode b)Hydrothermally grow ZnO nanorods from nanocrystalline seed layer c)Deposit polymer to infiltrate and cover rods d)Deposit and pattern gold top electrode e) Pattern polymer f) DRIE etch backside to release

The majority of the fabrication process leverages standard surface and bulk micromachining techniques, such as thermal oxidation, metal sputtering, photolithography (Figure 10) and deep reactive ion etching (DRIE). The challenge was to integrate those process steps with a novel process to create the nanocomposite material. Significant initial study went into researching and testing various nanorod growth techniques and polymer deposition methods and materials until we settled upon a combination that yielded dense vertical growth of high quality nanorods (Figure 11) and good polymer infiltration. The result was an ultrathin, highly compliant, low stress piezocomposite diaphragm that was compatible with the remaining process steps (Figure 12). Using this process, we have successfully fabricated several full wafers of sensors with decent yield.

There are two main ZnO nanorod growth methods, hydrothermal and VLS (vapor-liquid-solid) synthesis, Hydrothermal methods offer a relatively low temperature approach to synthesis, via immersion of a prepared substrate in a warm bath (~60 °C) of dilute zinc nitrate solution [9], [10]. By avoiding high temperatures, this approach thus allows for incorporation of an underlying polymer and bottom electrode, however for high quality nanorod growth on gold, a seed layer of ZnO nanocrystals needs to be deposited prior to growth.

The VLS (vapor-liquid-solid) method, on the other hand, takes a drastically different approach to nanorod synthesis, by utilizing a high temperature (800 °C – 900 °C) furnace for a gas-phase transport process using evaporation and condensation of Zn and oxygen vapors to form a ZnO nanostructure below a liquid catalyst metal [11].

After exploring these methods, we chose the hydrothermal approach, as the low processing temperatures enabled greater compatibility with the remainder of the fabrication process and generated lower residual stress on the thin film stack.

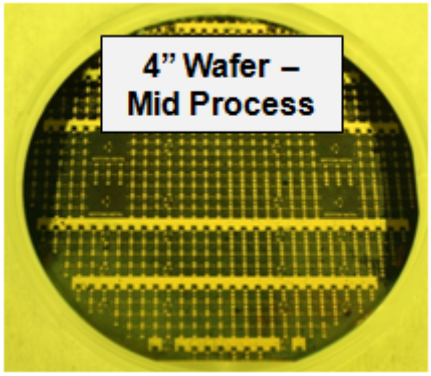

Figure 10: Photograph of 4" silicon wafer midway through the fabrication process. This wafer has a patterned bottom electrode and a grown array of vertical nanorods.

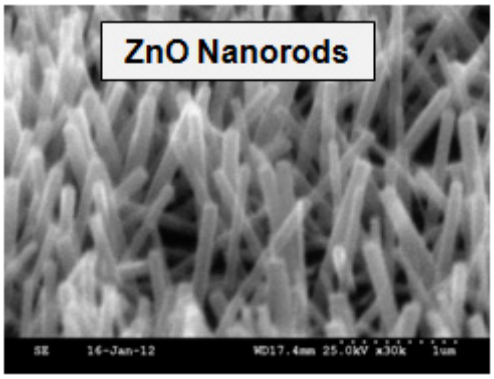

Figure 11: SEM image of ZnO nanorods grown directly on the gold electrode

Figure 12: Photograph of diaphragm from the backside after DRIE. A patterned gold bottom electrode is visible through the transparent diaphragm.

4.2. Packaging

Several different packaging schemes were explored during the initial characterization stages of the microphones. The first package, shown in Figure 11, was designed for basic microphone calibration inside an acoustic plane wave tube. The printed circuit board (PCB) length was extended to correctly mount the sensor inside the tube while providing coaxial electrical connection to the sensor output.

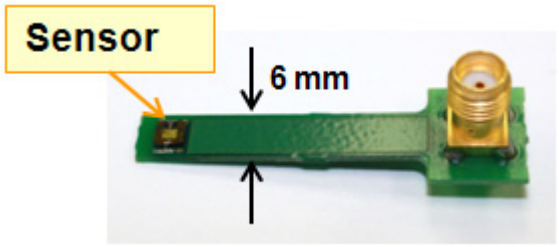

Figure 13: Photograph of microphone packaged on a simple PCB for benchtop testing.

After initial testing with the basic package, we designed and built a new package (Figure 12) that incorporates a co-located preamplifier to reduce noise and parasitic capacitance. We chose a Burr-Brown INA111 Instrumentation Amplifier as our preamplifier due to low input current noise and reasonable input voltage noise. Low input current noise is critical to maintain overall low noise performance when using high impedance sensors, such as these small piezoelectric microphones. The drawing and photograph also show the acoustic test fixture that allows us to mount the sensor directly at the end of an acoustic plane wave tube along with an adjacent reference microphone. Data and power was routed via ultrasmall MMCX-style coaxial connections.

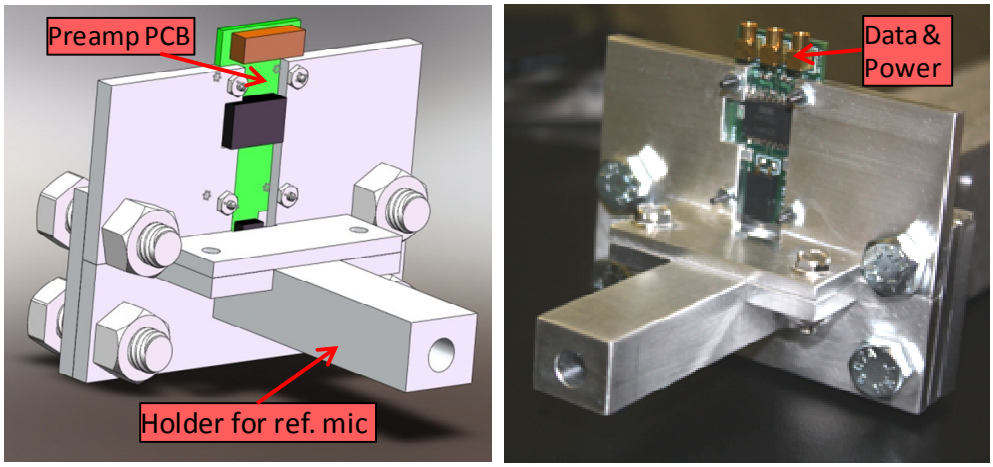

Figure 14: CAD drawing and photograph of microphone preamplifier package and acoustic test fixture.

5.0 Characterization

Several characterization methods were employed to understand and quantify the performance of the microphones. Electrical capacitance and resistance measurements provided a first look at some material properties and rapidly identified failed devices arising from electrical shorts. Acoustic tests were performed in an acoustic plane wave tube to provide a controlled, known acoustic input while measuring the output response of the sensors. Additional tests were performed under a laser vibrometer, using an applied voltage to actuate the microphones, yielding resonant frequency, mode shapes, and effective piezoelectric coefficients.

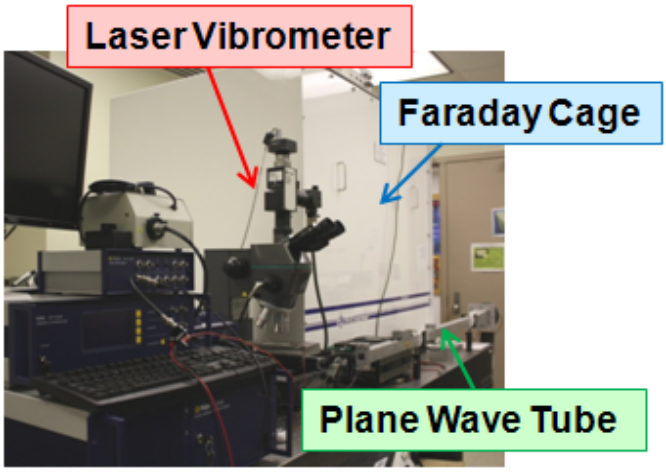

Figure 15: Photograph of experimental setup, highlighting acoustic plane wave tube, laser vibrometer and faraday shielded anechoic chamber.

5.1. Acoustic Characterization Setup

The fabricated devices were mounted at the end of an acoustic plane-wave tube, as shown in Figure 13 for dynamic calibration. The plane wave tube setup is used to measure sensitivity, linearity and frequency response of the microphones. The tube is designed to limit propagation of acoustic waves to the fundamental, planar mode at frequencies up to 16.88 kHz. A Bruel and Kjaer 4138, 1/8" pressure field microphone was also placed at the end of the tube to serve as a reference. A Bruel and Kjaer PULSE Analyzer was used to collect data from the sensor and a reference microphone. It also served as a signal source for driving a BMS acoustic compression driver via a Crown XTI-1000 Amplifier. A Stanford Research Systems SRS-560 preamplifier was used to amplify the sensor signal (from sensors mounted on the initial basic PCB) prior to data acquisition by the PULSE. Later tests using the preamplifer board eliminated the need for the SRS-560.

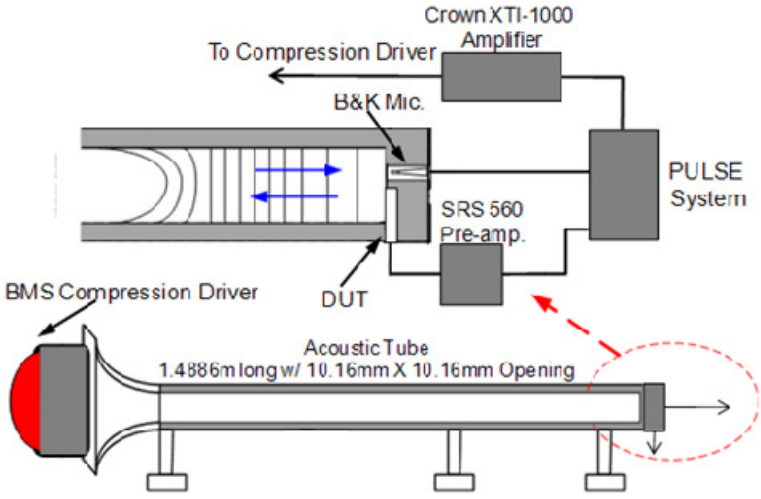

Figure 16: Schematic of acoustic plane wave tube setup.

5.2. Acoustic Characterization Results

Results from the acoustic tests (output voltage and sensitivity) for one sample sensor are shown in Figure 15 and Figure 16, respectively. This sensor, of Size 1, is our smallest sensor, having an outer radius of only 50 μm. Sensitivity was fairly constant (linear response) between 80 dBSPL and the upper end of our test at 112 dBSPL. The upper end of this range may extend beyond this but has not been tested yet (our setup allows for testing up to 150 dBSPL). The lower limit is defined by the noise floor of the sensor and is dominated by electrical thermal noise of the sensor (see Horowitz et al. [8] for an overview of piezoelectric noise sources).

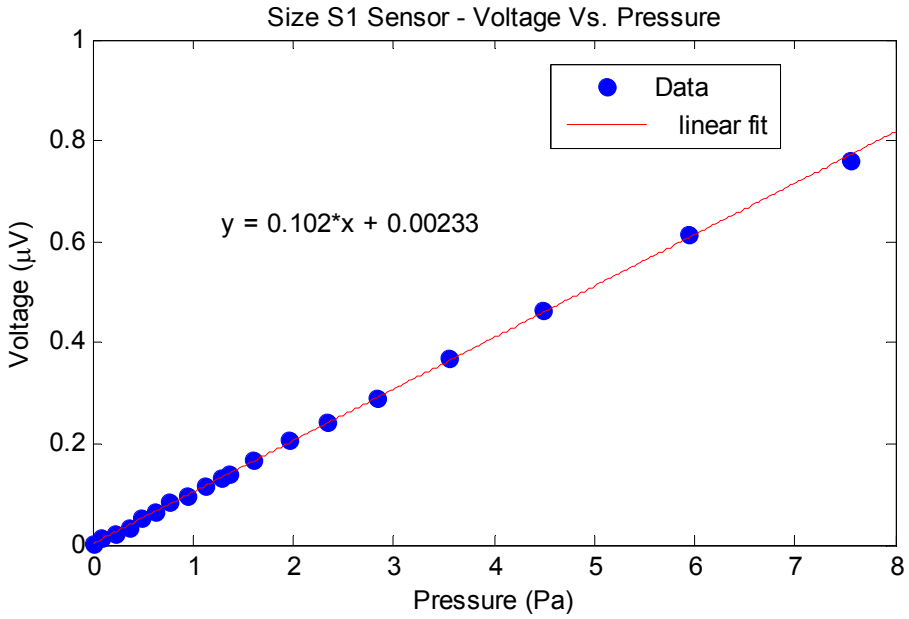

Figure 17: Measured output voltage (unamplified) versus applied acoustic pressure (in Pa).

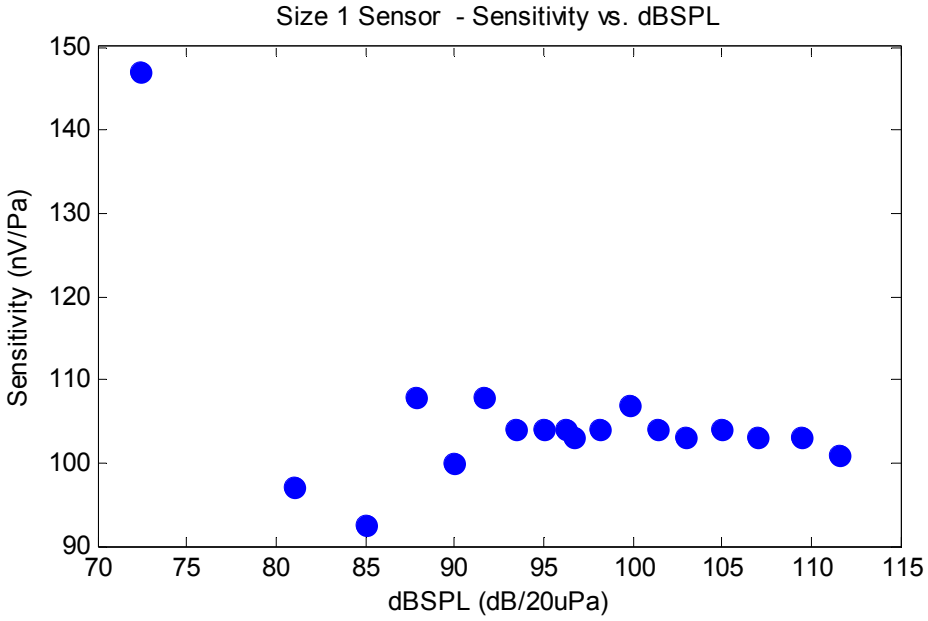

Figure 18: Measured sensitivity (unamplified) versus applied acoustic pressure (in dBSPL).

6.0 Conclusions and Future Work

Using a novel nanocomposite piezoelectric material, we have successfully developed and tested highly miniaturized piezoelectric microphones. Four different sensor sizes were designed and fabricated. Early results for the smallest of the sensors (50 μm radius) show functionality and reasonable performance. The measured sensitivity for this sample was 102 nV/Pa with a linear range from at least 80 to 112 dBSPL.

Further acoustic characterization is ongoing on all sensor sizes, using the 1 μm diaphragm thickness process. In addition, laser vibrometry is being performed to measure piezoelectric coefficients directly, along with mode shapes and resonant frequency (not testable acoustically due to plane-wave tube frequency limitations). We are also in the process of building up a statistical database of measured performance properties for all sensor sizes to understand device-to-device variation, long-term variation and fatigue issues and overall yield.

Future work will be focused on integrating these microphones into small arrays (single-chip and hybrid packaged) for beamforming and collision avoidance applications.

7.0 References

[1] R. Schellin, G. Hess, W. Kuehnel, G. M. Sessler, and E. Fukada, "Silicon Subminiature Microphones with Organic piezoelectric Layers," *IEEE Transactions on Electrical Insulation*, vol. 27, no. 4, pp. 867–871, 1992.

[2] R. P. Ried, S. Member, E. S. Kim, D. M. Hong, and R. S. Muller, "Piezoelectric Microphone with On-Chip CMOS Circuits," *Journal of Microelectromechanical Systems*, vol. 2, no. 3, pp. 111–119, 1993.

[3] J. Hillenbrand and G. M. Sessler, "Stacked piezoelectret microphones of simple design and high sensitivity," *IEEE Transactions on Dielectrics and Electrical Insulation*, vol. 13, no. 5, pp. 973–978, Oct. 2006.

[4] S. Horowitz, T. Nishida, L. Cattafesta, and M. Sheplak, "Development of a micromachined piezoelectric microphone for aeroacoustics applications.," *The Journal of the Acoustical Society of America*, vol. 122, no. 6, pp. 3428–36, Dec. 2007.

[5] S. B. Horowitz, D. Mathias, C. D. Hernandez, M. Sanghadasa, and P. Ashley, "Miniaturization of Piezoelectric Microphones," in *AIAA Infotech@Aerospace*, 2010.

[6] C. H. Ho, Y. M. Poon, and F. G. Shin, "New explicit formulas for the effective piezoelectric coefficients of binary 0-3 composites," *Journal of Electroceramics*, vol. 16, no. 4, pp. 283–288, Jul. 2006.

[7] Y. M. Poon, C. H. Ho, Y. W. Wong, and F. G. Shin, "Theoretical predictions on the effective piezoelectric coefficients of 0–3 PZT/Polymer composites," *Journal of Materials Science*, vol. 42, no. 15, pp. 6011–6017, Apr. 2007.

[8] S. B. Horowitz, A. D. Mathias, J. R. Fox, J. P. Cortes, M. Sanghadasa, and P. Ashley, "Effects of scaling and geometry on the performance of piezoelectric microphones," *Sensors and Actuators A: Physical*, vol. A185, pp. 24–32, 2012.

[9] J. W. P. Hsu, “Spatial organization of ZnO nanorods on surfaces via organic templating,” *Proceedings of SPIE*, vol. 5592, pp. 158–163, 2005.

[10] L. E. Greene, M. Law, J. Goldberger, F. Kim, J. C. Johnson, Y. Zhang, R. J. Saykally, and P. . Yang, “Low-temperature wafer-scale production of ZnO nanowire arrays.,” *Angewandte Chemie (International ed. in English)*, vol. 42, no. 26, pp. 3031–4, Jul. 2003.

[11] Z. Fan and J. G. Lu, “Zinc oxide nanostructures: synthesis and properties.,” *Journal of nanoscience and nanotechnology*, vol. 5, no. 10, pp. 1561–73, Oct. 2005.